Real or fake yellow in the vibrant colour craze: Rapid detection of lead chromate in turmeric

Sara W. Erasmus [a], Lisanne van Hasselt [a], Linda M. Ebbinge [b], Saskia M. van Ruth [a,b,*]

[a] *Food Quality and Design Group, Wageningen University and Research, P.O. Box 17, 6700 AA, Wageningen, the Netherlands*
[b] *Wageningen Food Safety Research, Wageningen University and Research, P.O. Box 230, 6700 AE, Wageningen, the Netherlands*

ARTICLE INFO

ABSTRACT

For centuries, the colour of foods has played a significant role in the way products are perceived and valued. Generally, the more vibrant the product, the higher its quality and price. For modern-day consumers, various brightly coloured foods are known as superfoods and often consumed at higher concentrations than before. There is emerging attention for adulteration of turmeric with the vibrant yellow, toxic and carcinogenic compound lead chromate. Rapid detection of this hazardous lead chromate is important to protect consumers, therefore this study aimed to develop a spectroscopy-based method to detect lead chromate in turmeric powder. The potential of Fourier transform-Raman (FT-Raman) spectroscopy was investigated experimentally by measuring multiple turmeric powder samples adulterated with different concentrations of lead chromate (0.1%–10.0%, w/w). The acquired FT-Raman spectra were analysed by both univariate and multivariate statistics. Linear correlation of the intensity of the main lead chromate Raman peak at 840 cm^{-1} against the lead chromate concentration gave a limit of detection (LOD) of 0.6%. For the partial least squares regression (PLSR) model, based on the 1750-200 cm^{-1} range, a LOD of 0.5% was obtained. Lead chromate was successfully detected for samples adulterated from 0.5% or higher. Raman spectroscopy is a promising screening technique for the rapid detection of lead chromate in turmeric powder at concentrations over 0.5%. However, the LOD for this study is still above the maximum levels that have been found in practice and future studies should focus on increasing the sensitivity of the technique.

1. Introduction

A food adulterant is a substance illegally added to food. Although food adulteration is generally known to be an intentional act, it is also an unintentional threat for food safety if the adulterants used are toxic. If a violation of the food law is committed intentionally to pursue economic gain through consumer deception, this is defined as food fraud (Spink & Moyer, 2011). Different types of food fraud exist, one being the addition of unapproved or undeclared substances. The latter can be added to conceal damage or inferiority of the raw materials and/or increase the bulk of the product; this is sometimes the case for the adulteration of turmeric.

Turmeric, predominantly grown in India, Bangladesh, Myanmar, China, and Nigeria, is a valuable spice, especially in South Asia, where it is consumed daily through culinary applications or medicinal practices to promote health (Prasad & Aggarwal, 2011, pp. 263–288). Its use as a food colouring and flavouring agent is essential to various well-known dishes; providing curry its characteristic yellow colour and flavour, while it is also used extensively for manufactured food products (i.e. dairy products, sauces, sweets, etc.). The vibrant yellow colour of

turmeric is one of the most desired quality attributes for gastronomic reasons, and therefore also the reason why this colour is preferred. Furthermore, this special product attribute acts as a motivation for fraudsters to adulterate turmeric with lead chromate.

In an early case, the Food and Drug Authority of India discovered 100–125 bags of turmeric laced with lead chromate in a manufacturing unit (Mishra, 2010). A recent study found that pregnant women in Bangladesh had high blood levels of lead (Pb) due to a yellow pigment (lead chromate) that was added to turmeric (Forsyth, Weaver, et al., 2019). The fraudulent addition takes place during the boiling and polishing steps when the outer skin is removed from the root (Forsyth, Nurunnahar, et al., 2019). The polishers add lead chromate (PbCrO₄) to the roots, due to its bright yellow colour, to satisfy wholesalers who prefer to sell vibrant turmeric as it is popular with consumers. The pigment is often provided to the polishers by the wholesalers. Additionally, lead chromate also hides any marks or damage to the roots. This is worrisome since lead chromate is a highly toxic and carcinogenic chemical, and it can cause damage to almost all functions of the human body (WHO, 2018). There is no evidence for a threshold of blood lead levels, below which no adverse health effects will occur (Lanphear et al., 2005). Therefore, it is very important that exposure to lead is prevented (Lanphear, 1998).

Media reports of turmeric adulteration with lead chromate often state that the adulteration occurred in the turmeric producing countries. Although this is true for some cases, it is important to bear in mind that there are also various other nodes of fraud vulnerability along the spice supply chain where adulteration can take place (Van Ruth, Luning, Silvis, Yang, & Huisman, 2018). The presence of lead chromate in turmeric is not solely a public health concern for South Asia, but also a concern for the Western world since the majority of turmeric is imported from Asia. Currently, the number one exporter of turmeric is India (CBI, 2016). In the last several years, the United States (U.S.) has recalled 13 brands of turmeric contaminated with Pb (Cowell, Ireland, Vorhees, & Heiger-Bernays, 2017). Also, in Europe, Pb and chromate (CrO_4^{2-}) were detected in turmeric powder, resulting in seizure (RASFF 2019.1832) or recall (RASFF 2017.0547) of the product. According to Forsyth, Nurunnahar, et al. (2019), it is likely that a lot of adulteration is overlooked by routine food safety tests.

Most of the colouring adulterants in herbs and spices are organic molecules with several aromatic rings (Reinholds, Bartkevics, Silvis, van Ruth, & Esslinger, 2015). In this respect, lead chromate is a special case as it is a metal salt. This chemical state affects its detection possibilities. A characteristic feature of lead chromate is the presence of the metals divalent lead (Pb(II)) and hexavalent chromium (Cr(VI)). These heavy metals can be targeted using X-ray fluorescence (XRF) and mass spectrometry techniques (Cowell et al., 2017; Forsyth, Nurunnahar, et al., 2019; Lin, Schaider, Brabander, & Woolf, 2010). The lead chromate content of turmeric is currently determined by inductively coupled plasma mass spectrometry (ICP-MS) (Cowell et al., 2017; Forsyth et al., 2018, 2019a, b). ICP-MS is time-consuming, involves elaborate sample preparation and skilled laboratory staff (Guimarães, Praamsma, & Parsons, 2016; Nordin & Selamat, 2013). Consequently, rapid detection strategies are needed. The Food Safety and Standard Authority of India provides consumers with a simple quick test where turmeric powder is added to water and the colour interpreted (FSSAI, 2012). However, it is subjective, while no quantitative value for the potential adulterant is provided. Non-destructive, rapid and simple methods would also be of value for determining lead chromate adulteration. The techniques commonly used to identify chemical adulterants in spices are mass spectrometry and spectroscopic methods (Osman et al., 2019; Varliklioz Er, Eksi-Kocak, Yetim, & Boyaci, 2017). Advantages of spectroscopic methods include their non-destructive nature, the minimal sample preparation needed before analysis and the high speed at which data is acquired.

Ultraviolet–visible (UV-VIS) spectroscopy can be used for coloured compounds, e.g., spice adulteration with Sudan dyes (Di Anibal, Odena,

Ruisánchez, & Callao, 2009). However, some drawbacks exist in using UV-VIS spectroscopy for the detection of lead chromate in turmeric. Lead chromate merely shows an absorption edge at a wavelength slightly higher than 500 nm, exhibiting no additional specific features in the UV-VIS range 400–700 nm (Cloutis, Norman, Cuddy, & Mann, 2016). Dissolution and dilution of the product are also needed for this technique. However, lead chromate has negligible solubility in water and it is questionable if a suitable solvent is available. Other promising spectroscopic methods include near-infrared (NIR) spectroscopy, infrared spectroscopy (IR) and Raman spectroscopy (Haughey, Galvin-King, Ho, Bell, & Elliott, 2015; Monago-Maraña et al., 2019). NIR spectroscopy is not a suitable method to detect lead chromate since chromates do not exhibit absorption bands in the 1100–2500 nm region (Cloutis et al., 2016). Besides, NIR spectroscopy used for adulterant identification showed inconsistencies between different laboratories (Osman et al., 2019). Cloutis et al. (2016) concluded that Raman or IR spectroscopy is more appropriate for the identification of chromate pigments. When using Fourier transform-infrared (FT-IR) spectroscopy, a characteristic peak for lead chromate can be found at 887 cm⁻¹ (11, 274 nm) (Desnica, Furic, Hochleitner, & Mantler, 2003). However, an FT-IR spectrum of pure curcumin also displays a peak at 887 cm⁻¹, this peak is the major colourant of turmeric (Dhakal et al., 2016). Besides, Raman spectroscopy was shown to be more sensitive to detecting lead chromate than FT-IR spectroscopy (Desnica et al., 2003). The Raman spectra of turmeric and pure curcumin do not contain an intense peak at 840 cm⁻¹ (11,905 nm); the characteristic peak for lead chromate (Dhakal et al., 2016). Lead chromates, including chrome yellow, are strong Raman scatterers. Raman spectroscopy was able to identify these pigments in cases where no infrared absorptions were observed (Suzuki & Carrabba, 2001). Thus, it can be concluded that Raman spectroscopy is the most promising spectroscopic screening technique for detecting lead chromate in turmeric.

Turmeric adulterated with lead chromate is receiving increasingly more attention in the scientific community as researchers gain insight into the specific adulteration practices. The next step in addressing and detecting this harmful adulteration practice is to develop a suitable and rapid screening technique. Current studies that have used Raman spectroscopy for the detection of turmeric adulteration, have only focused on its use to detect adulterants like starch and metanil yellow, but not to specifically detect lead chromate. Hence, the study is the first of its kind, to the best of the authors knowledge, that aims to explore the potential of FT-Raman spectroscopy to detect lead chromate in turmeric powder. The sensitivity of the detection technique will be determined, while a quantification model for the quantitative detection of lead chromate in turmeric powder will also be developed.

2. Materials and methods

2.1. Sample collection

Different batches of authentic turmeric powder were kindly donated by three independent and reputable European spice companies. The companies confirmed the authenticity and purity of the samples. Pure (98%) lead (II) chromate powder (Brunschwig Chemie BV, Amsterdam, the Netherlands) was used to prepare the adulterated samples.

2.2. Sample preparation and data acquisition

The investigation consisted of two parts. The first part of the study was performed to test the detectability of lead chromate in turmeric powder using one batch of turmeric and ten different levels of concentrations (procedure is specified below). In the second part of the study, a completely randomised experimental design was used to generate a large dataset for model development using 10 different batches of authentic turmeric powder each adulterated with seven different concentration levels of lead chromate as detailed below.

To investigate the detectability of lead chromate in turmeric powder by FT-Raman spectroscopy and to establish the concentration range to use for the model development part, authentic turmeric powder was adulterated with ten different concentration levels of lead chromate: 0%, 0.5%, 1.0%, 5.0%, 10.0%, 15.0%, 20.0%, 25.0%, 30.0%, 100% (w/w). Turmeric powder and lead chromate were weighed using an analytical balance. Powders were mixed by alternating shaking manually and vortexing horizontally. The exact mixing details are provided in Table S1 (Appendix A. Supplementary data). After mixing, the laced turmeric powder was transferred into clear 1 mL borosilicate glass VWR® vials (8.2 mm diameter, 40 mm height) (VWR®, Leuven, Belgium). Additionally, unadulterated turmeric powder and pure lead chromate were transferred directly to the VWR® vials. The powder was then pressed (by using the back of a spoon) to obtain a pellet which gives a higher spectral intensity and prevents sedimentation due to differences in particles size. Each sample was prepared in triplicate and analysed. The sample preparation procedure as described above was followed for all samples.

In part two of the study, a larger data set suitable for further model development was generated. Ten different batches of authentic turmeric powder were used to prepare the adulterated samples of the lower concentrations 0%, 0.1%, 0.5%, 1.0%, 2.5%, 5.0% and 10.0% (w/w). This resulted in 10 (batches) x 7 (concentrations) x 3 (sample replicates) = 210 (n) samples. The three sample replicates prepared for each sample were averaged to minimize the influence of variability in mixing. Hence, the means of 70 samples were used for further data analysis.

2.3. Raman spectroscopy

FT-Raman spectra of the samples were recorded using a RAM II FT-Raman Module (Bruker Nederland B.V, Leiderdorp, The Netherlands) coupled to a VERTEX 70 FT-IR spectrometer, equipped with a 1064 nm laser. Curcumin, a major component in turmeric, exhibits native fluorescence (Peng, Zeng, Zhou, Lian, & Nie, 2015). The interference of strong fluorescence can be limited by using laser light in the near-infrared range, especially 1064 nm as used in this study (Schulz & Baranska, 2006). The VWR® vials containing the sample material were clamped in the sample holder with a small mirror positioned behind the samples to reflect the light. The spectra were recorded at 4 cm^{-1} resolution in the range from 50 to 3600 cm^{-1}, obtaining an average of 32 successive scans. The laser power was set at 500 mW. For each sample vial, three spectra were recorded. The VWR® vial was rotated after the recording of each spectrum so that each measurement was taken from a different side (new position) of the vial. The three spectra per sample vial (analysis replicate) were averaged for data analysis.

2.4. Pre-processing of spectral data

The Unscrambler X10.5 software (version 10.5, Camo Software AS, Oslo, Norway) was used for pre-processing of the FT-Raman spectral data. Spectra of the three replicates (per sample) were averaged, resulting in reduced noise signal. Pre-processing is used to minimize variability in the acquired spectra. However, applying too much pre-processing steps can result in a loss of information (Oliveira, Cruz-Tirado & Barbin, 2019). It is important to limit the number of pre-processing steps to preserve valuable information and develop a model which is robust enough for future predictions (Rinnan, van den Berg, & Engelsen, 2009). In Table S2 (Appendix A. Supplementary data), an overview is given of commonly applied pre-processing steps in the analysis of Raman spectra of adulterated powdered foods. These methods were used as a guideline for testing and running various pre-processing techniques, of which the most promising techniques were selected for the study.

According to Afseth, Segtnan, and Wold (2006), applying sequentially baseline correction, normalization, using a reduced data region, the range that contains the spectral information, and mean centering,

lead to the best calibration model of biological samples. They concluded that smoothing led to loss of intensity. Yet, for the detection of adulterated onion powder, the best results were obtained by second order polynomial curve fitting, a baseline correction method, followed by first derivative Sawiztky–Golay (SG) for noise removal (Lee, 2015). Since averaging of three replicate spectra reduced the noise considerably, smoothing was considered unnecessary for this study. The 1750 to 200 cm^{-1} range displayed only considerable baseline offset. This baseline offset was corrected by applying a linear baseline correction. This eliminated the need to use the commonly applied baseline correction method that uses a polynomial curve fitting (Liland, Kohler, & Afseth, 2016). Since normalization and mean centering are especially important to make spectra comparable for quantification, these techniques were also applied to the spectra of this study.

2.5. Data analysis

The pre-processed mean spectra (per sample) were used for data analysis. Data analysis was performed using Unscrambler X10.5 and XLSTAT® statistical software (Version 2019.3.2; Addinsoft, NY, USA; https://www.xlstat.com). All analyses were performed on the preprocessed spectral range of 1750–200 cm^{-1}. As qualitative tests, principal component analysis (PCA) and linear discriminant analysis (LDA) were used, while univariate linear correlation and partial least squares regression (PLSR) were carried out as quantitative analyses. PCA (Cowe & McNicol, 1985) was used to visualize the grouping of samples of different concentrations, and any trends in the data. LDA was performed to generate a classification model between authentic and adulterated samples. The linear correlation and PLSR models were built to predict the lead chromate concentration based on the FT-Raman spectra. For univariate calibration models, the limit of detection (LOD) and limit of quantification (LOQ) can correspondingly be calculated by the equations: 3.3 x σ/S and 10 x σ/S, where σ is the standard deviation of the y-intercept and S the slope of the calibration curve (EMEA, 2006). The same approach was applied to the PLSR calibration models of this study (Sezer, Bilge, Berkkan, Tamer, & Hakki Boyaci, 2018).

3. Results and discussion

In Raman spectroscopy, monochromatic light, generated by the high intensity laser, is pointed towards a sample. The photons collide with the sample molecules which are then excited to higher virtual energy levels. If a molecule relaxes back to its initial energy state, a photon with the same frequency of the light source is scattered (Rayleigh scatter). However, a few molecules relax to another vibrational state, resulting in scattered photons of a different wavelength (Raman scatter) (Rodriguez-Saona, Ayvaz, & Wehling, 2017). The specific frequencies depend on the chemical bonds present in the molecules. In a Raman spectrum, each peak corresponds to a specific molecular bond vibration. Thus, a Raman spectrum is a chemical fingerprint of the sample analysed. Since peak intensity is directly proportional to the concentration, Raman spectroscopy is suitable for both qualitative and quantitative analyses.

3.1. Spectral interpretation and detectability of lead chromate in turmeric powder

The first part of the study explored the detectability of lead chromate in turmeric powder by FT-Raman spectroscopy using a wide range of concentrations. This initial step was crucial to establish if the method can detect lead chromate, if there are any interferences due to the way the sample is analysed (through VWR® vials), and to determine the lowest concentration level that could be further explored. In Fig. 1, the raw Raman spectra of turmeric powder laced with different concentrations of lead chromate (a), the spectrum of the VWR® vial (b), the spectrum of pure turmeric powder (c), and the spectrum of pure lead chromate (d) are shown. Since the range 1750–200 cm^{-1} contains all the
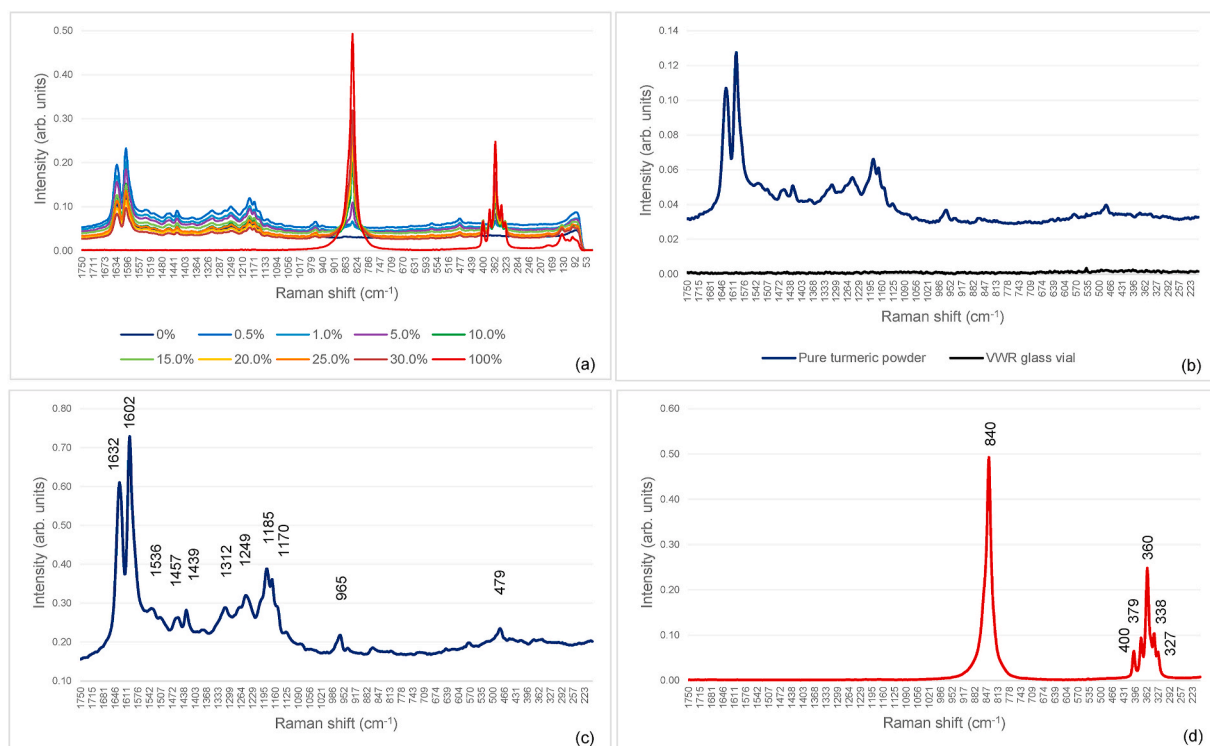
Fig. 1. The (a) raw FT-Raman spectra of turmeric powder laced with different concentrations (0%, 0.5%, 1.0%, 5.0%, 10.0%, 15.0%, 20.0%, 25.0%, 30.0%, 100%; each represented by a different colour) of lead chromate, (b) spectrum of the VWR vial compared to a pure turmeric powder spectrum, (c) spectrum of pure turmeric powder, and (d) spectrum of pure lead chromate recorded at 200 mW laser power. X-axis: Raman shift (cm^{-1}); Y-axis: Intensity (arbitrary units). (For interpretation of the references to colour in this figure, the reader is referred to the web version of this paper).

important spectral information (Fig. 1a), only this range was used to further process the spectra.

Due to safety reasons, it was necessary to record the Raman spectra through VWR® vials. It is possible to record Raman spectra through containers as measuring through containers could add some noise but would not interfere with the characteristic fingerprints (Vašková, 2011). Similar results were obtained in this study. Except for some additional noise, the borosilicate glass did not influence the measurements negatively (Fig. 1b). Measuring the samples directly will result in less noise and thus give a higher Signal to Noise Ratio (S/N), resulting in lower detection limits. The measurement through VWR® vials also had an advantage as it enabled higher laser powers to be used, thereby increasing spectral intensity without burning the sample. This positive outcome means that future analyses can limit safety concerns due to the handling of potentially contaminated samples by simply analysing the samples through VWR® vials.

Fig. 1c and d shows the spectra of the authentic turmeric powder and pure lead chromate, respectively. In Fig. 1d, the highest intensity FT-Raman peak is located at 840 cm^{-1}, and the collection of smaller peaks at 400, 379, 360, 338 and 327 cm^{-1}. This spectrum is the same as the lead chromate reference spectrum provided by CAMEO Chemicals (2019). In fact, the signal at 840 cm^{-1} corresponds to symmetric stretching of CrO_4^{2-}, while the other peaks correspond to bending modes of CrO_4^{2-} (Frost, 2004). The authentic (unadulterated) turmeric powder spectrum (Fig. 1c) does not contain any major peaks at these wavenumbers and is a promising result for the use of FT-Raman for the detection of adulterated samples. The assignment of the major turmeric powder bands to vibrational modes are shown in Table 1.

Fig. 2 shows the range 1750–200 cm^{-1}, to which a linear baseline correction (Fig. 2b) has been applied. The 100% sample indicates the FT-Raman spectral fingerprint of pure lead chromate (Fig. 2a). The laced turmeric powder samples exhibit characteristic lead chromate peaks at the same wavenumbers. It is evident that the intensity of the

Table 1
The assignment of major turmeric FT-Raman bands to vibrational modes.

Raman shift (cm^{-1})	Assignment (Dhakal et al., 2016)	Assignment (Kolev, Velcheva, Stamboliyska, & Spiteller, 2005)
1632	v (disubstituted C=C)	v (C=C); v (C=O)
1602	v (C=C)	v (C=C); v (C=O)
1536	δ(Ar–O + Ar–O–R)	v (C=O); δ(CC[10]C); δ(CC=O)
1457		δ(CH$_3$)[B]
1430		δ(CCC)[Ph]; δ(CCH)[Ph]; δ(COH)[A]
1312		δ(C-Ph); δ(CCH)[Ph(B)]
1249	CH bending	δ(CCH)[Ph(A)]; δ(COH)[A]
1185	CH$_3$ deformation	δ(CH$_3$)[B]; δ(CC[16]H)
1170	CH bending	δ(CH$_3$)[A]; δ(COH)[A]; δ(CCH)[scel]
965	= CH wag trans	δ(CC[13]H); v (C=O); δ(CC[15]H)

Vibrational modes: (ν) stretching; (δ) in-plane bending; (Ph) aromatic ring vibrations; (A) vibrations connected with the 'enolic' part of the molecule; (B) vibrations connected with the 'keto' part of the molecule.

characteristic lead chromate peaks increases with increasing lead chromate concentration, while the intensity of the turmeric powder peaks decreases. Even the lower concentrations appear to give a lead chromate signal. The intensity of the prominent 840 cm^{-1} peak against lead chromate concentration can be described by a linear correlation as shown in Fig. 2b.

3.2. Evaluation of lead chromate in turmeric powder

The raw spectra of 10 batches of turmeric powder adulterated at seven low concentrations of lead chromate, 0%, 0.1%, 0.5%, 1.0%, 2.5%, 5.0% and 10.0% (w/w), are shown in Fig. 3a. The raw spectra show a considerable degree of difference in the baseline offset, while spectra of the same concentration levels are not aligned. After the application of a linear baseline correction and normalization, the concentration levels are clearly grouped (Fig. 3b), and an increase can be
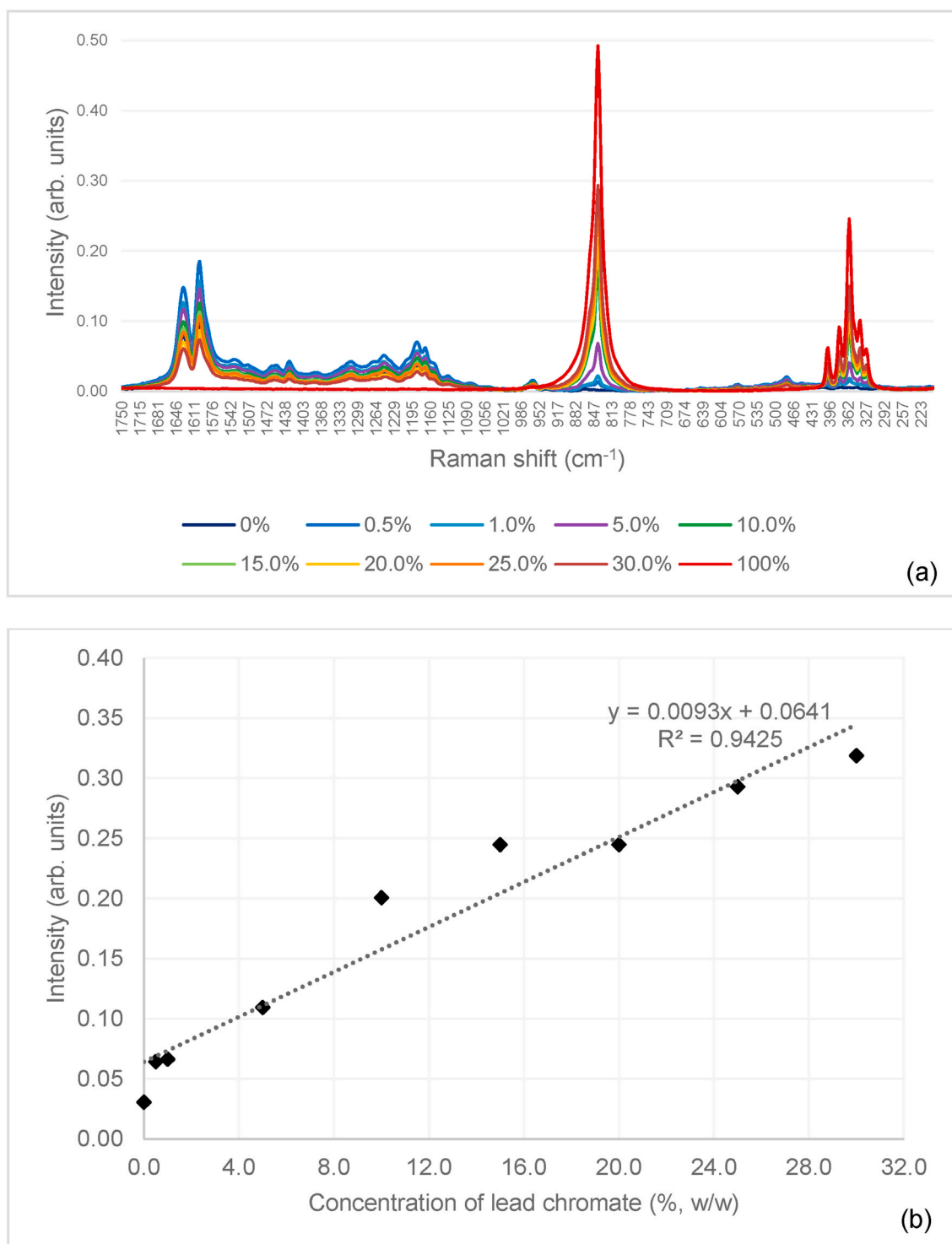
Fig. 2. The (a) baseline corrected FT-Raman spectra of the region 1750-200 cm^{-1} (concentrations of lead chromate added to turmeric powder: 0%, 0.5%, 1.0%, 5.0%, 10.0%, 15.0%, 20.0%, 25.0%, 30.0%, 100%; each represented by a different colour), and (b) the intensity of the characteristic 840 cm^{-1} Raman peak against lead chromate concentration (%, w/w). X-axis: Raman shift (cm^{-1}); Y-axis: Intensity (arbitrary units). (For interpretation of the references to colour in this figure, the reader is referred to the web version of this paper).

seen in signal intensity with increasing levels of lead chromate adulteration at the characteristic wavenumbers (i.e. 840, 400, 379, 360, 338 and 327 cm^{-1}).

3.2.1. Qualitative analysis by PCA and LDA

A first exploration using PCA shows that the adulterated samples of 2.5%, 5.0% and 10.0% lead chromate are clearly separated from each

other (Fig. S1; Appendix A. Supplementary data). The samples with lower concentrations are overlapping, hence it cannot be determined yet (based on the PCA) if the concentrations below 2.5% can be discriminated from pure turmeric powder samples. In the loadings line plot for principal component 1 (PC-1) (Fig. S1), both the turmeric powder (prominent positive peaks at 1632 and 1602 cm^{-1}) and the major lead chromate (prominent negative peaks at 840 and 360 cm^{-1}) are reflected.
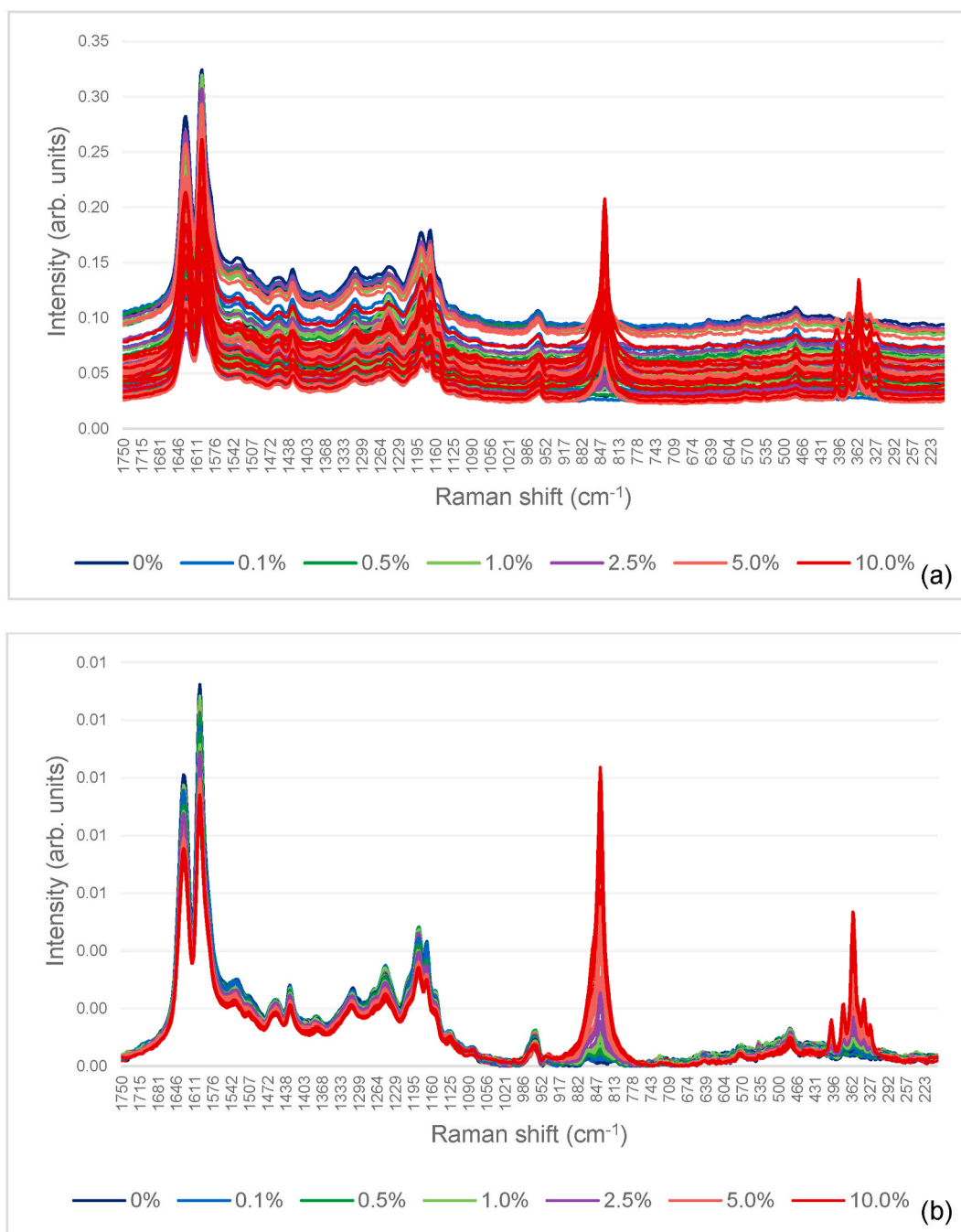
Fig. 3. The (a) raw FT-Raman spectra of turmeric powder laced with different concentrations (0%, 0.1%, 0.5%, 1.0%, 2.5%, 5.0% and 10.0%; each represented by a different colour) of lead chromate, and (b) the graph of the linear baseline corrected and normalized spectra. X-axis: Raman shift (cm^{-1}); Y-axis: Intensity (arbitrary units). (For interpretation of the references to colour in this figure, the reader is referred to the web version of this paper).

This is in line with the observed separation of the groups along PC-1 of the scores plot, where the samples with higher concentrations of lead chromate (2.5%, 5.0%, 10.0%) are located on the left (negative) side of the plot, and the samples with lower concentrations of lead chromate (0%, 0.1%, 0.5%, 1.0%) on the right (positive) side of the plot. The former samples produced signals with higher intensities at the characteristic wavenumbers of lead chromate, while the latter samples produced higher intensities at the characteristic wavenumbers of turmeric.

Linear discriminant analysis was investigated as a tool to discriminate between adulterated and unadulterated (authentic) samples. The PCA-scores were used since the data set contains more variables than samples. The best model performance was obtained using the Mahalanobis method and analysing two components. The analysis was performed on both the entire 1750-200 cm^{-1} range and the selected ranges (907-782 cm^{-1}, 404-396 cm^{-1}, 383-321 cm^{-1}) which include the characteristic lead chromate peaks (Table 2). By only analysing the lead chromate ranges, a slightly higher accuracy could be obtained. False negatives are the most problematic, as the samples are then assumed to be safe while it contains very toxic lead chromate. All false negatives were samples containing the lowest concentration 0.1% (w/w) lead chromate. This result means that only concentrations of 0.5% (w/w) and higher can be classified correctly using this technique.

3.3. Quantitative analysis by linear correlation

For the targeted detection of lead chromate, the known spectral

Table 2

Linear discriminant analysis (LDA) classification using the Mahalanobis method of authentic and adulterated turmeric powder samples based on two spectral ranges (range 1: 1750-200 cm-1; range 2: 907-782 cm-1, 404-396 cm-1, 383-321 cm-1).

Spectral range	Actual	Classified[a]		
		Authentic	Adulterated	Total
Range 1	Authentic	**8**	2	10
	Adulterated	4	**56**	60
% Correctly classified		80	93	**91**
Range 2	Authentic	**8**	2	10
	Adulterated	2	**58**	60
% Correctly classified		80	97	**94**

Mahalanobis method: two components used; (%) Percentage; [a] The number of correctly classified observations (in bold) are tabulated diagonally.

features of the adulterant can be used for a univariate analysis approach. The intensity of the highest (representative) peak at 840 cm^{-1} is linearly correlated to the lead chromate concentration (Fig. 4) (y = 0.0008x + 0.0002; R^2 = 0.990). The samples with the higher concentrations of lead chromate have more variation. However, this is not a major issue since only very low concentrations of lead chromate, i.e. 0.2% (w/w) or lower, are added in practice. During the weighing of the lead chromate, particles displayed static behaviour. This static behaviour may have caused deviations in the 'real' adulteration concentration. Furthermore, variation between samples could be caused by an inhomogeneous

distribution of lead chromate particles over the turmeric powder. Since the Raman laser scans only a small spot of sample material, the measurements are sensitive to this inhomogeneity. The small laser spot size can be overcome by using hyperspectral Raman imaging. This is of serious importance as spices are often heterogeneously contaminated (BfR, 2016). This method has already been applied to detect metanil yellow in turmeric powder (Chao, Dhakal, Qin, Kim, & Peng, 2018).

Using the linear correlation model (Fig. 2b), an LOD and LOQ value of respectively 0.6% and 1.9% (w/w) were calculated. The Pb concentrations in turmeric analysed by Cowell et al. (2017) were between 0.03 and 99.50 mg/kg, while Forsyth, Nurunnahar, et al. (2019) found concentrations up to 1152 mg/kg. The latter is equivalent to 1798 mg/kg lead chromate in turmeric powder; ~0.2% (w/w) (PubChem, 2019). This study's detection limit was 0.5–0.6% (w/w) (discrimination by LDA and linear correlation). Therefore, this limit means that the sensitivity of the current method needs to be improved to be used in practice.

3.3.1. Quantitative analysis by PLSR

Fig. 2 shows that the intensity of the characteristic lead chromate peaks increases with increasing concentration. Therefore, it was investigated whether a model that predicts the lead chromate concentration based on the acquired spectrum can be generated. In Figs. S2 and S3 (Appendix A. Supplementary data), two PLSR models are shown based on different spectral ranges (range 1: 1750-200 cm^{-1}; range 2: 907-782 cm^{-1}, 404-396 cm^{-1}, 383-321 cm^{-1}). A quantitative prediction model based on the whole 1750-200 cm^{-1} range (Fig. S2: R^2 = 0.913; RMSE =
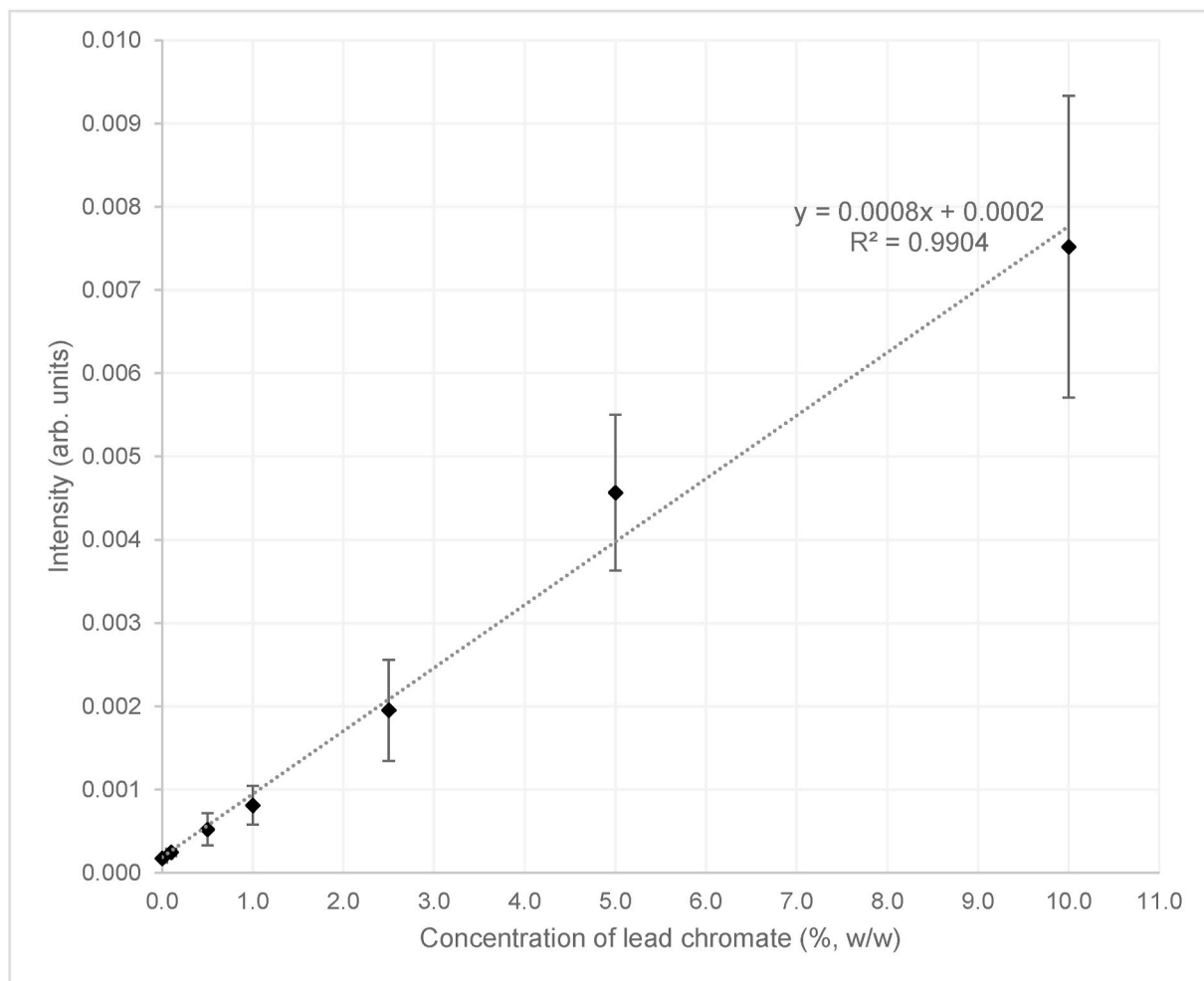

Fig. 4. The linear correlation between FT-Raman spectral peak (840 cm^{-1}) intensity (in arbitrary units) and lead chromate concentration (%, w/w) with standard deviation error bars.

0.993) performs similarly to the lead chromate specific ranges (Fig. S3: $R^2 = 0.909$; RMSE = 1.044); nonetheless the R^2 is slightly higher and the root mean square error (RMSE) slightly lower for the whole range. This is probably because the characteristic turmeric and lead chromate signals contribute towards the model's predictive power. The size of the regression coefficients gives an indication of which variables have an important impact on the response variables. The B coefficients (as shown in Fig. S2c,d and S3c,d) are calculated from the raw data table and used for predictions. From the loadings and regression coefficient plots (Fig. S2), it is evident that the distinct peaks for turmeric (i.e. the most prominent at 1632 and 1602 cm^{-1}) and lead chromate (840 and 400, 379, 360, 338 and 327 cm^{-1}) have the highest regression coefficients and thus, influence the model the most. This is the clearest for factor-1, which describes 88% of the variance. For the other PLSR model (range 2), the lead chromate peaks are the determining variables, as these are present in the selected wavenumber range (factor-1 describes 91% of the variance). Given the interferences of the turmeric peaks that can influence the model, it might be best to use the lead chromate specific ranges when this model is used to predict the adulteration of turmeric varieties not included in this research.

The LOD (%, w/w) of PLSR range 1 and 2 was 0.5, while the LOQ (%, w/w) was 1.5 for both models. For the models, 92% (range 1) and 93% (range 2) is explained by only two factors; making them fairly robust. The moderately high RMSE reflects the variability between samples of the same concentration, already mentioned before. For future studies, it is recommended to prepare a larger sample set, including more turmeric powder varieties (with more external variation) to make the model more robust. The variability could also be diminished by ensuring better mixing. If these requirements are met, the predictive power of this model can be tested. For the mixing of turmeric powder with starch, Kar, Tudu, Jana, and Bandyopadhyay (2019) used a high-speed ultrasonicator to ensure homogeneity. However, this also affects the particle size variation. Consequently, using an ultrasonicator would not reflect the desired practice of FT-Raman to be directly applied on the material without prior sample preparation.

3.4. General considerations for the detectability of lead chromate in turmeric powder

The study demonstrated the potential of FT-Raman spectroscopy for the development of a rapid screening technique to detect lead chromate in turmeric. It is promising given that the characteristic spectral fingerprints of both lead chromate and turmeric is clearly distinguishable at different FT-Raman bands (as discussed in section 3.1). Furthermore, the VWR® vials (used due to safety concerns) did not interfere with the measurement, but enhanced it, and can therefore be easily used in future analyses.

During the initial planning stages of the study, various other spectroscopy techniques were considered as they are increasingly used for rapid screening and fraud detection. Yet, to specifically target lead chromate in turmeric, several methods were found to be unsuitable (Cloutis et al., 2016; Desnica et al., 2003; Dhakal et al., 2016): ultraviolet–visible (UV-VIS) spectroscopy displays no characteristic lead chromate features in the UV-VIS range 400–700 nm; chromates do not exhibit absorption bands in the 1100–2500 nm region using near-infrared (NIR) spectroscopy; Fourier transform-infrared (FT-IR) spectroscopy displays a characteristic peak for both lead chromate and pure curcumin at 887 cm^{-1}. Raman spectroscopy does not have these drawbacks, making it a promising spectroscopic screening technique for lead chromate in turmeric (as shown in the study). Yet, one should also consider new technological developments, particularly for sensor technologies and portable devices, that could offer other promising detection and screening techniques in the future.

Safety was a huge concern during the study as the handling of the lead chromate posed several risks. Following a risk assessment, protocols for proper handling of the materials and performance of the experiments were developed. This imposed restrictions for the type of analytical scales that could be used and handled. Consequently, lower adulteration levels could not be tested due to the nature of the product (powder) as this would have resulted in a higher inaccuracy of the level of adulteration. Dissolution and dilution of the product was also problematic as lead chromate has negligible solubility in water and it is questionable if a suitable solvent is available for these purposes as it is known to be only soluble in diluted nitric acid. A way to solve this would be to use facilities specifically designed for the handling of hazardous materials. Also, future research could adopt an alternative approach: acquisition of adulterated batches or suspected batches, e.g., by extremely low price or samples that have been confiscated by authorities, and subsequent measurement of lead chromate content by both FT-Raman spectroscopy and a confirmatory technique such as ICP-MS (Reinholds et al., 2015). In this way, the challenge of adulterating turmeric powder accurately (for developing prediction models) is circumvented, while any deviation can be corrected for through the confirmatory analyses.

An aspect of the current FT-Raman method that needs further attention is the detection sensitivity. Alternative approaches, like emerging dispersive Raman instruments, resonance Raman and surface-enhanced Raman spectroscopy (SERS) could solve this problem. An enhanced signal and lower detection limits could be obtained with emerging dispersive 1064 nm Raman instruments (Gallimore, Davidson, Kalberer, Pope, & Ward, 2018). In resonance Raman, the laser's wavelength is tuned to match the energy of a relevant electronic transition. This gives a large increase in scattering intensity by factor 10^2-10^6. However, it is questionable whether a frequency exists where fluorescence by turmeric does not dominate. Wei, Chen, and Liu (2015) state that resonance Raman can lead to signals dominating fluorescence. Efremov, Ariese, and Gooijer (2008) describe why fluorescence is very likely to interfere with resonance Raman emission. With SERS, the Raman scattering signal is increased (Jensen, Aikens, & Schatz, 2008) and the fluorescence effects quenched (Kögler, Itkonen, Viitala, & Casteleijn, 2020; Wei et al., 2015) through the interaction between sample molecules and a metallic nanostructure. Under optimal conditions the amplification could reach a factor 10^{11} or even 10^{15} (López, Ruisánchez, & Callao, 2013). Although SERS requires sample preparation by depositing the sample on a substrate, it could be useful to detect adulterants at trace levels.

The method developed in this study, for both LDA and PLSR algorithms, were only able to detect adulteration levels of 0.5% (w/w), 5000 mg/kg, and higher. These LODs are quite distant from the target LOD (as stipulated by regulations or standards), and from what is seen in real practice. Although, no limits for hexavalent chromium, Cr(VI), in foods are specified (EFSA, 2014), there are regulations for heavy metal contaminants. The maximum permissible limit of Pb in spices, established by the U.S. Department of Agriculture (USDA), is 2 mg/kg (Ward & Huong, 2013). The Agmark standard states that turmeric powder should not contain any chromate, while Pb should be below a maximum of 2.5 mg/kg (Plotto, Mazaud, Röttger, & Steffel, 2004). Reinholds et al. (2015) and Reinholds, Pugajeva, Bavrins, Kuckovska, and Bartkevics (2017) took as a guideline a maximum limit of 0.3 mg/kg Pb in condiments, based on EU regulations and FAO standards. Hence, it would be ideal if a rapid technique could detect at such low levels. Using the current method, increasing its sensitivity and utilising a portable, handheld version, it might be possible to pick out the worst of the worst.

4. Conclusions

This study investigated the rapid detection of lead chromate in turmeric powder. FT-Raman spectroscopy, with a 1064 nm laser, showed great potential for rapid detection with minimal sample preparation. Multivariate, as well as univariate statistical analyses, were employed to process the spectral data. With LDA, turmeric powder adulterated with concentrations of 0.5% (w/w) or higher could be

discriminated from authentic/unadulterated samples. The highest accuracy was obtained when the model was based on the lead chromate specific ranges. Based on the linear correlation of the intensity of the major 840 cm^{-1} FT-Raman peak against concentration, a LOD of 0.6% (w/w) was calculated. Concerning PLSR, a model based on the 1750-200 cm^{-1} range resulted in the best performance, with a LOD of 0.5% (w/w). To increase the robustness of the models, turmeric powder from different origins (to increase sample size and variation) should also be included in future studies. Ultimately, the wider the differences in turmeric samples, the more accurate the model becomes. Future research should focus on increasing the sensitivity of the technique so that the low lead chromate concentrations added in practice can be detected. Then, this rapid screening tool would be a valuable contribution to the mitigation of food fraud and the protection of public health.

CRediT authorship contribution statement

Sara W. Erasmus: Conceptualization, Methodology, Resources, Writing - original draft, Writing - review & editing, Supervision. **Lisanne van Hasselt:** Conceptualization, Methodology, Formal analysis, Investigation, Writing - original draft, Writing - review & editing. **Linda M. Ebbinge:** Methodology, Writing - review & editing. **Saskia M. van Ruth:** Conceptualization, Resources, Writing - review & editing, Supervision, Project administration, Funding acquisition.

Declaration of competing interest

The authors declare that there is no conflict of interest.

Acknowledgements

Appendix A. Supplementary data

Supplementary data to this article can be found online at https://doi.org/10.1016/j.foodcont.2020.107714.

References

Afseth, N. K., Segtnan, V. H., & Wold, J. P. (2006). Raman spectra of biological samples: A study of preprocessing methods. *Applied Spectroscopy, 60*(12), 1358–1367. https://doi.org/10.1366/000370206779321454
Bundesinstitut für Risikobewertung (BfR) (Federal Institute for Risk Assessment). (2016). *Final Report Summary - SPICED (Securing the spices and herbs commodity chains in Europe against deliberate, accidental or natural biological and chemical contamination) (Issue: June).* https://cordis.europa.eu/project/id/312631/reporting.
CBI. (2016). *Exporting curcuma longa (turmeric) to Europe.* https://www.cbi.eu/market-information/natural-ingredients-health-products/curcuma-longa-turmeric/. (Accessed 30 April 2020).
Chao, K., Dhakal, S., Qin, J., Kim, M., & Peng, Y. (2018). A 1064 nm dispersive Raman spectral imaging system for food safety and quality evaluation. *Applied Sciences, 8*(3), 431. https://doi.org/10.3390/app8030431
Chemicals, C. A. M. E. O. (2019). *Lead chromate.* https://cameochemicals.noaa.gov/chemical/20564. (Accessed 3 December 2019).
Cloutis, E., Norman, L., Cuddy, M., & Mann, P. (2016). Spectral reflectance (350-2500 nm) properties of historic artists' pigments. II. Red–orange–yellow chromates, jarosites, organics, lead(-tin) oxides, sulphides, nitrites and antimonates. *Journal of Near Infrared Spectroscopy, 24*(2), 119–140.

Cowell, W., Ireland, T., Vorhees, D., & Heiger-Bernays, W. (2017). Ground turmeric as a source of lead exposure in the United States. *Public Health Reports, 132*(3), 289–293. https://doi.org/10.1177/0033354917700109
Cowe, I. A., & McNicol, J. W. (1985). The use of principal components in the analysis of near-infrared spectra. *Applied Spectroscopy, 39*(2), 257–265. https://doi.org/10.1366/0003702854248944
Desnica, V., Furic, K., Hochleitner, B., & Mantler, M. (2003). A comparative analysis of five chrome green pigments based on different spectroscopic techniques. *Spectrochimica Acta Part B: Atomic Spectroscopy, 58*(4), 681–687. https://doi.org/10.1016/S0584-8547(02)00283-5
Dhakal, S., Chao, K., Schmidt, W., Qin, J., Kim, M., & Chan, D. (2016). Evaluation of turmeric powder adulterated with metanil yellow using FT-Raman and FT-IR Spectroscopy. *Foods, 5*(2), 36. https://doi.org/10.3390/foods5020036
Di Anibal, C. V., Odena, M., Ruisánchez, I., & Callao, M. P. (2009). Determining the adulteration of spices with Sudan I-II-II-IV dyes by UV–visible spectroscopy and multivariate classification techniques. *Talanta, 79*(3), 887–892.
Efremov, E. V., Ariese, F., & Gooijer, C. (2008). Achievements in resonance Raman spectroscopy. Review of a technique with a distinct analytical chemistry potential. *Analytica Chimica Acta, 606*(2), 119–134. https://doi.org/10.1016/j.aca.2007.11.006
EMEA. (2006). ICH topic Q2 (R1). Validation of analytical procedures: Text and methodology. CPMP/ICH/381/95) https://www.ema.europa.eu/en/documents/scientific-guideline/ich-q-2-r1-validation-analytical-procedures-text-methodology-step-5_en.pdf. (Accessed 30 April 2020).
European Food Safety Authority (EFSA). (2014). EFSA Panel on Contaminants in the Food Chain. Scientific opinion on the risks to public health related to the presence of chromium in food and drinking water. *EFSA Journal, 12*(3). https://doi.org/10.2903/j.efsa.2014.3595
Food Safety and Standard Authority of India (FSSAI). (2012). *Quick test for some adulterants in food. Instruction manual - part II (methods for detection of adulterants)* Accessed http://old.fssai.gov.in/Portals/0/Pdf/Final_Test_kit_Manual_II%2816-08-2012%29.pdf. (Accessed 30 April 2020).
Forsyth, J. E., Nurunnahar, S., Islam, S. S., Baker, M., Yeasmin, D., Islam, M. S., et al. (2019b). Turmeric means "yellow" in Bengali: Lead chromate pigments added to turmeric threaten public health across Bangladesh. *Environmental Research, 179,* 108722. https://doi.org/10.1016/j.envres.2019.108722
Forsyth, J. E., Saiful Islam, M., Parvez, S. M., Raqib, R., Sajjadur Rahman, M., Marie Muehe, E., et al. (2018). Prevalence of elevated blood lead levels among pregnant women and sources of lead exposure in rural Bangladesh: A case control study. *Environmental Research, 166,* 1–9. https://doi.org/10.1016/j.envres.2018.04.019
Forsyth, J. E., Weaver, K. L., Maher, K., Islam, M. S., Raqib, R., Rahman, M., et al. (2019a). Sources of blood lead exposure in rural Bangladesh. *Environmental Science & Technology, 53*(19), 11429–11436. https://doi.org/10.1021/acs.est.9b00744
Frost, R. L. (2004). Raman microscopy of selected chromate minerals. *Journal of Raman Spectroscopy, 35*(2), 153–158.
Gallimore, P. J., Davidson, N. M., Kalberer, M., Pope, F. D., & Ward, A. D. (2018). 1064 nm Dispersive Raman microspectroscopy and optical trapping of pharmaceutical aerosols. *Analytical Chemistry, 90*(15), 8838–8844. https://doi.org/10.1021/acs.analchem.8b00817
Guimarães, D., Praamsma, M. L., & Parsons, P. J. (2016). Evaluation of a new optic-enabled portable X-ray fluorescence spectrometry instrument for measuring toxic metals/metalloids in consumer goods and cultural products. *Spectrochimica Acta Part B: Atomic Spectroscopy, 122,* 192–202. https://doi.org/10.1016/j.sab.2016.03.010
Haughey, S. A., Galvin-King, P., Ho, Y. C., Bell, S. E. J., & Elliott, C. T. (2015). The feasibility of using near infrared and Raman spectroscopic techniques to detect fraudulent adulteration of chili powders with Sudan dye. *Food Control, 48,* 75–83. https://doi.org/10.1016/j.foodcont.2014.03.047
Jensen, L., Aikens, C. M., & Schatz, G. C. (2008). Electronic structure methods for studying surface-enhanced Raman scattering. *Chemical Society Reviews, 37*(5), 1061–1073. https://doi.org/10.1039/b706023h
Kar, S., Tudu, B., Jana, A., & Bandyopadhyay, R. (2019). FT-NIR spectroscopy coupled with multivariate analysis for detection of starch adulteration in turmeric powder. *Food Additives & Contaminants: Part A, 36*(6), 863–875. https://doi.org/10.1080/19440049.2019.1600746
Kögler, M., Itkonen, J., Viitala, T., & Casteleijn, M. G. (2020). Assessment of recombinant protein production in E. coli with time-gated surface enhanced Raman spectroscopy (TG-SERS). *Scientific Reports, 10*(1). https://doi.org/10.1038/s41598-020-59091-3
Kolev, T. M., Velcheva, E. A., Stamboliyska, B. A., & Spiteller, M. (2005). DFT and experimental studies of the structure and vibrational spectra of curcumin. *International Journal of Quantum Chemistry, 102*(6), 1069–1079. https://doi.org/10.1002/qua.20469
Lanphear, B. P. (1998). The paradox of lead poisoning prevention. *Science, 281*(5383), 1617–1618. https://doi.org/10.1126/science.281.5383.1617
Lanphear, B. P., Hornung, R., Khoury, J., Yolton, K., Baghurst, P., Bellinger, D. C., et al. (2005). Low-level environmental lead exposure and children's intellectual function: An international pooled analysis. *Environmental Health Perspectives, 113*(7), 894–899. https://doi.org/10.1289/ehp.7688
Lee, S., Lohumi, S., Lim, H. S., Gotoh, T., Cho, B. K., Kim, M. S., et al. (2015). Development of a detection method for adulterated onion powder using Raman spectroscopy. *Journal of the Faculty of Agriculture, 60*(1), 151–156. Kyushu University.
Liland, K. H., Kohler, A., & Afseth, N. K. (2016). Model-based pre-processing in Raman spectroscopy of biological samples. *Journal of Raman Spectroscopy, 47*(6), 643–650. https://doi.org/10.1002/jrs.4886

Lin, C. G., Schaider, L. A., Brabander, D. J., & Woolf, A. D. (2010). Pediatric lead exposure from imported Indian spices and cultural powders. *Pediatrics, 125*(4), e828–e835. https://doi.org/10.1542/PEDS.2009-1396

López, M. I., Ruisánchez, I., & Callao, M. P. (2013). Figures of merit of a SERS method for Sudan I determination at traces levels. *Spectrochimica Acta Part A: Molecular and Biomolecular Spectroscopy, 111*, 237–241. https://doi.org/10.1016/j. saa.2013.04.031

Mishra, A. (2010). *This food could be injurious to health*. The Times of India. https://times ofindia.indiatimes.com/city/kanpur/This-food-could-be-injurious-to-health/arti cleshow/5914081.cms. (Accessed 30 April 2020).

Monago-Maraña, O., Eskildsen, C. E., Afseth, N. K., Galeano-Díaz, T., Muñoz de la Peña, A., & Wold, J. P. (2019). Non-destructive Raman spectroscopy as a tool for measuring ASTA color values and Sudan I content in paprika powder. *Food Chemistry, 274*, 187–193. https://doi.org/10.1016/j.foodchem.2018.08.129

Nordin, N., & Selamat, J. (2013). Heavy metals in spices and herbs from wholesale markets in Malaysia. *Food Additives and Contaminants: Part B, 6*(1), 36–41. https:// doi.org/10.1080/19393210.2012.721140

Oliveira, M. M., Cruz-Tirado, J. P., & Barbin, D. F. (2019). Nontargeted analytical methods as a powerful tool for the authentication of spices and herbs: A review. *Comprehensive Reviews in Food Science and Food Safety, 18*(3), 670–689. https://doi. org/10.1111/1541-4337.12436

Osman, A. G., Raman, V., Haider, S., Ali, Z., Chittiboyina, A. G., & Khan, I. A. (2019). Overview of analytical tools for the identification of adulterants in commonly traded herbs and spices. *Journal of AOAC International, 102*(2), 376–385. https://doi.org/ 10.5740/jaoacint.18-0389

Peng, Q., Zeng, C., Zhou, Y., Lian, S., & Nie, G. (2015). Rapid determination of turmeric roots quality based on the Raman spectrum of curcumin. *Food Analytical Methods, 8* (1), 103–108. https://doi.org/10.1007/s12161-014-9874-y

Plotto, A., Mazaud, F., Röttger, A., & Steffel, K. (2004). *Turmeric: Post-production management*. FAO. http://www.fao.org/fileadmin/user_upload/inpho/docs/Pos t_Harvest_Compendium_-_Turmeric.pdf. (Accessed 30 April 2020).

Prasad, S., & Aggarwal, B. B. (2011). Turmeric, the golden spice: From traditional medicine to modern medicine. In *Herbal medicine: Biomolecular and clinical aspects* (2nd ed., p. 288). CRC Press.

PubChem. (2019). *Lead chromate*. https://pubchem.ncbi.nlm.nih.gov/compound/Lead -chromate. (Accessed 30 April 2020).

Reinholds, I., Bartkevics, V., Silvis, I. C. J., van Ruth, S. M., & Esslinger, S. (2015). Analytical techniques combined with chemometrics for authentication and determination of contaminants in condiments: A review. *Journal of Food Composition and Analysis, 44*, 56–72. https://doi.org/10.1016/j.jfca.2015.05.004

Reinholds, I., Pugajeva, I., Bavrins, K., Kuckovska, G., & Bartkevics, V. (2017). Mycotoxins, pesticides and toxic metals in commercial spices and herbs. *Food Additives and Contaminants: Part B, 10*(1), 5–14. https://doi.org/10.1080/ 19393210.2016.1210244

Rinnan, Å., van den Berg, F., & Engelsen, S. B. (2009). Review of the most common pre-processing techniques for near-infrared spectra. *Trends in Analytical Chemistry, 28* (10), 1201–1222.

Rodriguez-Saona, L., Ayvaz, H., & Wehling, R. L. (2017). Infrared and Raman spectroscopy. In S. Nielsen (Ed.), *Food analysis* (pp. 107–127). Cham: Springer. https://doi.org/10.1007/978-3-319-45776-5_8.

Schulz, H., & Baranska, M. (2006). Rapid evaluation of quality parameters in plant products applying ATR-IR and Raman spectroscopy. *Acta Horticulturae, 1*(712), 347–356.

Sezer, B., Bilge, G., Berkkan, A., Tamer, U., & Hakki Boyaci, I. (2018). A rapid tool for determination of titanium dioxide content in white chickpea samples. *Food Chemistry, 240*, 84–89. https://doi.org/10.1016/j.foodchem.2017.07.093

Spink, J., & Moyer, D. C. (2011). Defining the public health threat of food fraud. *Journal of Food Science, 76*(9), R157–R163. https://doi.org/10.1111/j.1750-3841.2011.02417.x

Suzuki, E. M., & Carrabba, M. (2001). *In situ* identification and analysis of automotive paint pigments using line segment excitation Raman spectroscopy: I. Inorganic topcoat pigments. *Journal of Forensic Sciences, 46*(5), 1053–1069.

Van Ruth, S. M., Luning, P. A., Silvis, I. C. J., Yang, Y., & Huisman, W. (2018). Differences in fraud vulnerability in various food supply chains and their tiers. *Food Control, 84*, 375–381. https://doi.org/10.1016/j.foodcont.2017.08.020

Varliklioz Er, S., Eksi-Kocak, H., Yetim, H., & Boyaci, I. H. (2017). Novel spectroscopic method for determination and quantification of saffron adulteration. *Food Analytical Methods, 10*(5), 1547–1555. https://doi.org/10.1007/s12161-016-0710-4

Vašková, H. (2011). A powerful tool for material identification: Raman spectroscopy. *International Journal of Mathematical Models and Methods in Applied Sciences, 5*(7), 1205–1212. http://www.naun.org/main/NAUN/ijmmas/17-120.pdf.

Ward, M., & Huong, B. (2013). *Technical regulations on mycotoxin and heavy metals MRLs in foods*. https://gain.fas.usda.gov/Recent GAIN Publications/Technical Regulations on Mycotoxin and Heavy Metals MRLs in Foods _Hanoi_Vietnam_12-10-2013.pdf. (Accessed 30 April 2020).

Wei, D., Chen, S., & Liu, Q. (2015). Review of fluorescence suppression techniques in Raman spectroscopy. *Applied Spectroscopy Reviews, 50*(5), 387–406. https://doi.org/ 10.1080/05704928.2014.999936

World Health Organization (WHO). (2018). *Lead*. https://www.who.int/ipcs/assessment /public_health/lead/en/. (Accessed 30 April 2020).